Dalton Transactions

ROYAL SOCIETY OF CHEMISTRY

PAPER

View Article Online
View Journal | View Issue

Cite this: *Dalton Trans.*, 2024, **53**, 753

Enhancing isoprene polymerization with high activity and adjustable monomer enchainment using cyclooctyl-fused iminopyridine iron precatalysts†

Nighat Yousuf,[a,b,c] Yanping Ma, *[a] Qaiser Mahmood, *[b] Wenjuan Zhang, *[d] Yizhou Wang,[a,c] Hassan Saeed[a,b,c] and Wen-Hua Sun *[a,b,c]

In this study, a series of structurally rigid cyclooctyl-fused iminopyridine iron complexes, $[L_2FeCl][FeCl_4]$ and $[2L_3Fe][Cl][3FeCl_4]$, was synthesized *via* a one-pot method and investigated as precatalysts in conjunction with methylaluminoxane for isoprene (Ip) polymerization. Combined characterization through FTIR analysis, elemental analysis and single crystal XRD analysis fully verified the structure of these complexes. The most active iron complex, **Fe^{H}**, exhibited a trisligated nature, with its cation adopting an octahedral geometry around the metal center. In contrast, all the other iron complexes (**Fe^{2Me}**, **Fe^{2Et}**, **Fe^{2iPr}**, **Fe^{3Me}**, **Fe^{2Et,Me}**) displayed bisligated configurations, with distorted trigonal bipyramidal geometry of cations. During isoprene polymerization, the extent of steric hindrance of the ligand framework exerted a significant impact on catalytic performance. The **Fe^{H}** precatalyst with less steric hindrance demonstrated excellent performance, producing high molecular weight polyisoprenes with conversions exceeding 99% for 4000 equiv. of monomer. Even at very low catalyst loadings, as low as 0.0025 mol% (Fe/Ip), the polymerization of isoprene could proceed smoothly with an exceptionally high activity of 4.0×10^6 g_{PI} $(mol_{Fe}, h)^{-1}$. Moreover, this precatalyst exhibited good thermal stability, maintaining high activity levels (typically 10^5 g_{PI} $(mol_{Fe}, h)^{-1}$) across a broad temperature range from −20 °C to 100 °C. Additionally, by adjusting steric substituents and the reaction temperature, the 1,4/3,4 regioselectivity could be modulated from 9/91 to 69/31 while maintaining a high stereoselectivity of *cis*-1,4 structures (*cis*/*trans*: >99/1).

Received 3rd November 2023,
Accepted 29th November 2023

DOI: 10.1039/d3dt03674j

rsc.li/dalton

Introduction

Metal catalytic polymerization of isoprene may afford various polyisoprene (PI) configurations, including *cis*-1,4, *trans*-1,4, 3,4 (isotactic, syndiotactic, atactic) and the less common 1,2 (isotactic, syndiotactic, atactic).[1] Polyisoprenes (PI) with these distinct configurations exhibit versatile chemical, thermal and physical properties, rendering them valuable for a wide array of applications such as rubber manufacturing, shape memory technology, the pharmaceutical industry, *etc.*[2] The catalyst structure is crucial for producing highly selective polyisoprenes. Recent advancements in the catalyst structure have even enabled the synthesis of polyisoprene structures closely resembling natural rubber.[3] PI with high *trans*-1,4 selectivity possesses crystalline and tough characteristics comparable to balata and gutta-percha rubbers, while *cis*-1,4 PI, resembling *Hevea brasiliensis* latex, offers elasticity with lower crystallinity.[4,5] Over the various polymerization methods, including radical, cationic, and anionic processes, it is possible to fine-tune the stereo- and regioselectivity of the polymer microstructure, to a certain extent, through coordination–insertion polymerization. The

[a]*Key Laboratory of Engineering Plastics and Beijing National Laboratory for Molecular Science, Institute of Chemistry, Chinese Academy of Sciences, Beijing 100190, China. E-mail: whsun@iccas.ac.cn, myanping@iccas.ac.cn*
[b]*Chemistry and Chemical Engineering Guangdong Laboratory, Shantou 515031, China. E-mail: qaiser@ccelab.com.cn*
[c]*CAS Research/Education Center for Excellence in Molecular Sciences and International School, University of Chinese Academy of Sciences, Beijing 100049, China*
[d]*Beijing Key Laboratory of Clothing Materials R&D and Assessment, School of Materials Science and Engineering, Beijing Institute of Fashion Technology, Beijing 100029, China. E-mail: zhangwj@bift.edu.cn*

†Electronic supplementary information (ESI) available: General consideration and materials, the procedure for isoprene polymerization, X-ray crystallographic studies, and Table S1. Crystal data and structure refinement for **Fe^{H}**, **Fe^{2Me}** and **Fe^{2Et,Me}**, and Fig. S1–S22. ^{1}H and ^{13}C NMR spectra for entry 3, Table 1; entries 2–10 and 12–14, Table 2; entries 2–5, Table 3; entries 2–5, Table 4. CCDC 2305303 (**Fe^{H}**), 2305304 (**Fe^{2Me}**) and 2305305 (**Fe^{2Et,Me}**). For ESI and crystallographic data in CIF or other electronic format see DOI: https://doi.org/10.1039/d3dt03674j

degree of control mainly depends on the ligand structure with fine tuning through steric and electronic factors.[2,3]

Classical catalysts, such as $TiCl_4$/alkylaluminum, lithium organic, and neodymium catalysts, are widely used for producing *cis*-1,4 PI.[6] In contrast, the vanadium trichloride/triethylaluminum catalytic system is efficient for the synthesis of *trans*-1,4 PI.[7] Over the past two decades, the development of new well-defined transition metal catalysts afforded not only highly selective PI, but also introduced new microstructures of polyisoprene featuring a diverse sequence of 1,4 and 3,4 additions.[8] Among them, iron catalysts are preferred for use due to their high metal abundance, cost-effectiveness, low toxicity, ease of preparation, and stability under a wide range of polymerization conditions.[9] However, there were few reports on iron precatalysts for isoprene polymerization until the 2000s.[10] Iron complexes bearing aromatic N,N bidentate ligand structures in combination with alkyl aluminum cocatalysts have emerged as highly active catalysts for isoprene polymerization, with high 3,4 selectivity (**A**, Fig. 1).[11] Thus, N, N bidentate-Fe(II) catalysts have recently gained significant attention for their remarkable activity, selectivity, living characteristics (in some cases) and the ability to polymerize various conjugated dienes.[12] The discovery of α-diimine-nickel/-palladium catalysts in 1995 and bis(imino)pyridine-iron/cobalt catalysts in 1998 for ethylene polymerization marked a significant milestone in catalyst development for olefin and diene polymerization (**B**, Fig. 1).[13] In these efforts, Ritter and coworkers reported iminopyridine iron complexes as highly active catalysts for isoprene polymerization. These complexes bearing *N*-octyl (**C**, Fig. 1) or *N*-aryl (**D**, Fig. 1) imine moieties afford *trans*-1,4 or *cis*-1,4 polyisoprene, respectively.[14] Subsequently, Chen *et al.* demonstrated alkyl and disubstituted aryl variants of iminopyridine iron complexes for isoprene polymerization, providing high molecular weight polyisoprenes predominantly consisting of *cis*-1,4 units.[15] More recently, Ricci and coworkers modified these catalysts with mono-substituted *N*-aryl units and achieved polyisoprenes with a preference for *cis*-1,4 and 3,4 alternating microstructures, in which *cis*-1,4 structures were in a sequence of 3 or 5 units.[8d,16] Wang *et al.* examined aminopyridine iron precatalysts in which the *N*-aryl group was extensively modified with various alkyl and aryl substituents, aiming to fine-tune the monomer enchainment (**E**, Fig. 1). These iron precatalysts notably favored the addition of the 3,4-unit monomer, accounting for approximately 50% of the product, while displaying high activity levels reaching up to 1.9×10^6 g_{PI} $(mol_{Fe}, h)^{-1}$.[12e] Visseaux and coworkers incorporated the methyl group at the imine carbon (**F**, Fig. 1), resulting in high polymerization activities ($>2.1 \times 10^7$ g_{PI} $(mol_{Fe}, h)^{-1}$), tunable regioselectivity (up to 1,4/3,4: 9/1), and stereoselectivity of polyisoprene (up to *cis*-1,4/*trans*-1,4: >99/0).[17] In recent research, our group introduced a novel class of π-conjugated naphthalenyl-substituted iminopyridine iron precatalysts, which exhibited remarkable catalytic activity, reaching up to 5.5×10^5 g_{PI} $(mol_{Fe}, h)^{-1}$, and high molecular weight polyisoprenes with tunable selectivity (**G**, Fig. 1).[18] Fusion of the carbocyclic ring at C2 and C3 carbon of pyridine exhibited dramatic effects on the polymerization behaviour, significantly enhancing activities and thermal stability (**H** and **I**, Fig. 1). For instance, incorporation of cyclohexyl significantly improved the activities up to 1.0×10^8 g_{PI} $(mol_{Fe}, h)^{-1}$ with high thermal stability and produced high molecular weight polyisoprenes with tunable stereochemistry (**H**, Fig. 1).[19] These outcomes are even more pronounced when transitioning to larger carbocyclic rings, such as cycloheptyl (**I**, Fig. 1). In this case, the polymerization activity experiences a notable boost, reaching 1.2×10^8 g_{PI} $(mol_{Fe}, h)^{-1}$ and the resulting polyisoprenes consistently maintain high molecular weights (typically 10^5 g mol^{-1}) across all reaction temperatures within the range of 25 °C to 100 °C.[20] These exciting results highlight the potential of iron catalysts

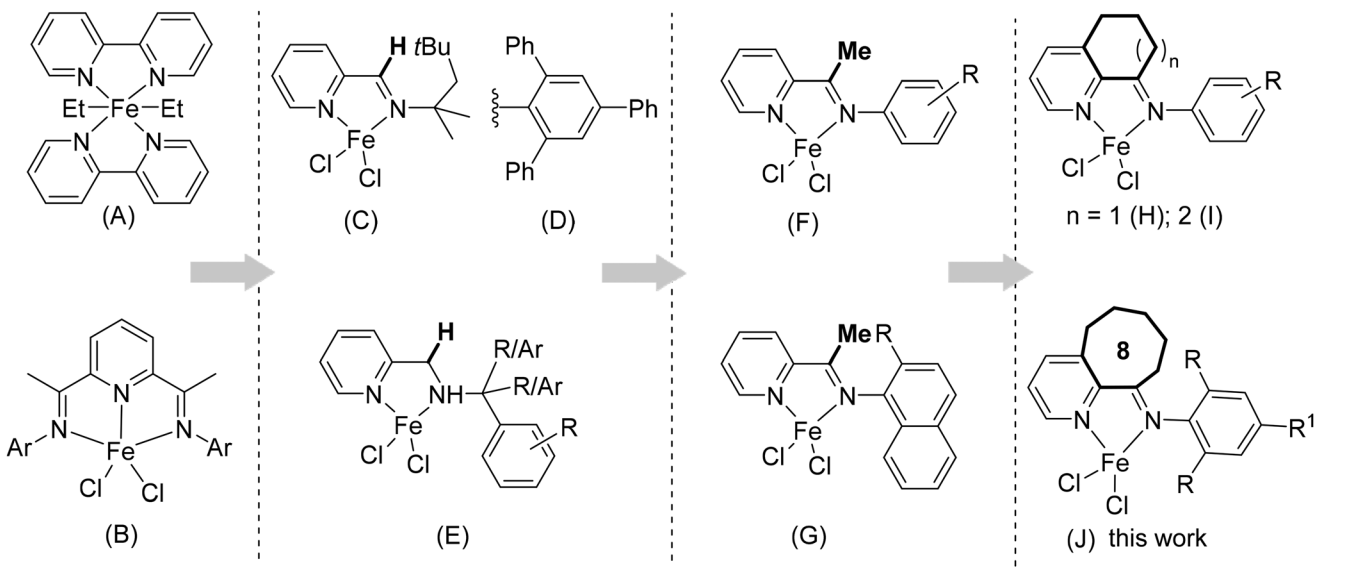

Fig. 1 Structural variations in iminopyridine iron precatalysts for isoprene polymerization.

to replace classical titanium-based and rare earth metal catalysts for isoprene polymerization. However, it is essential to simultaneously improve polymerization activities, selectivity, and polymer molecular weights and control dispersity under conditions critical for industrial applications.

Motivated by the results of incorporating carbocyclic rings into iminopyridine iron catalysts for ethylene polymerization, our objective was to investigate the effects of using even larger rings on the catalytic performance of iron catalysts in isoprene polymerization.[21] Herein, we synthesized a series of cyclooctyl-fused iminopyridine iron precatalysts specifically designed for isoprene polymerization (**J**, Fig. 1) and systematically investigated the influence of various reaction conditions (cocatalyst type and amount, temperature, reaction time, catalyst and monomer quantities) and the impact of the ligand structure on the polymerization performance. The results revealed that, besides the key role of the catalyst structure in determining the polymerization activities, the monomer enchainment (predominantly *cis*-1,4/3,4) in the produced polyisoprene could be tuned by adjusting the steric substituents and reaction temperature. Furthermore, the high thermal stability and prolonged life of active species were clearly evident from parallel reactions conducted over a wide range of temperatures and run times. To gain a thorough understanding and characterization of the prepared complexes and the resulting polymer, a comprehensive analysis using various methods and techniques was performed.

Results and discussion

Synthesis and characterization of iron complexes

The iron complexes $[L_2FeCl][FeCl_4]$, where L = 10-(alkylphenylimino)-5,6,7,8,9-pentahydrocycloocta[*b*]pyridine [alkyl = 2,6-dimethyl (**Fe^{2Me}**), 2,6-diethyl (**Fe^{2Et}**), 2,6-isopropyl (**Fe^{2iPr}**), 2,4,6-trimethyl (**Fe^{3Me}**), 2,6-diethyl-4-methyl (**$Fe^{2Et,Me}$**)], and $[2L_3Fe][Cl][3FeCl_4]$ where L = 10-(phenylimino)-5,6,7,8,9-pentahydrocycloocta[*b*] pyridine (**Fe^{H}**), were prepared using a straightforward one-pot template method, eliminating the need for tedious synthesis and purification of ligands, as depicted in Scheme 1.[2d,18,19,22] The synthesis involved the reaction of 5,6,7,8,9-pentahydrocycloocta[*b*]pyridine-10-one, iron chloride, and aniline in acetic acid at boiling temperature, affording the corresponding iron complexes in high yields. Characterization of these compounds revealed an unexpected oxidation–reduction reaction, leading to ion pairs: $[L_2FeCl][FeCl_4]$ and $[2L_3Fe][Cl][3FeCl_4]$, where L represents the ligand structure.[15,18,23] FTIR analysis, elemental analysis, and single crystal X-ray diffraction analysis verified the structures, as shown in Scheme 1. The cation of the **Fe^{H}** complex is trisligated, while the cations of all other complexes are bisligated. Their FTIR spectra showed the absorption of the imine functional group in the range of 1635–1621 cm^{-1} which are slightly lower in value than those reported for the ligands in the literature.[21b] Meanwhile, the results of elemental analysis data are also supportive of their structures. Similar oxidation reactions have been previously reported for iron complexes.[15,18,23]

Single crystals of **Fe^{H}**, **Fe^{2Me}** and **$Fe^{2Et,Me}$**, suitable for X-ray determinations, were grown through the slow diffusion of *n*-hexane into a solution of the corresponding complexes in dichloromethane at room temperature. The molecular structures of these complexes demonstrated an ion pair configuration, with **Fe^{H}** featuring a trisligated iron cation and **Fe^{2Me}** and **$Fe^{2Et,Me}$** exhibiting bisligated iron chloride cations. Perspective views of these three complexes are given in Fig. 2 and 3, respectively, along with key bond lengths and angles in the figure captions.

In the molecular structure of the **Fe^{H}** cation, six nitrogen atoms originating from three ligands form a geometry that can be best described as an octahedron around the iron center,

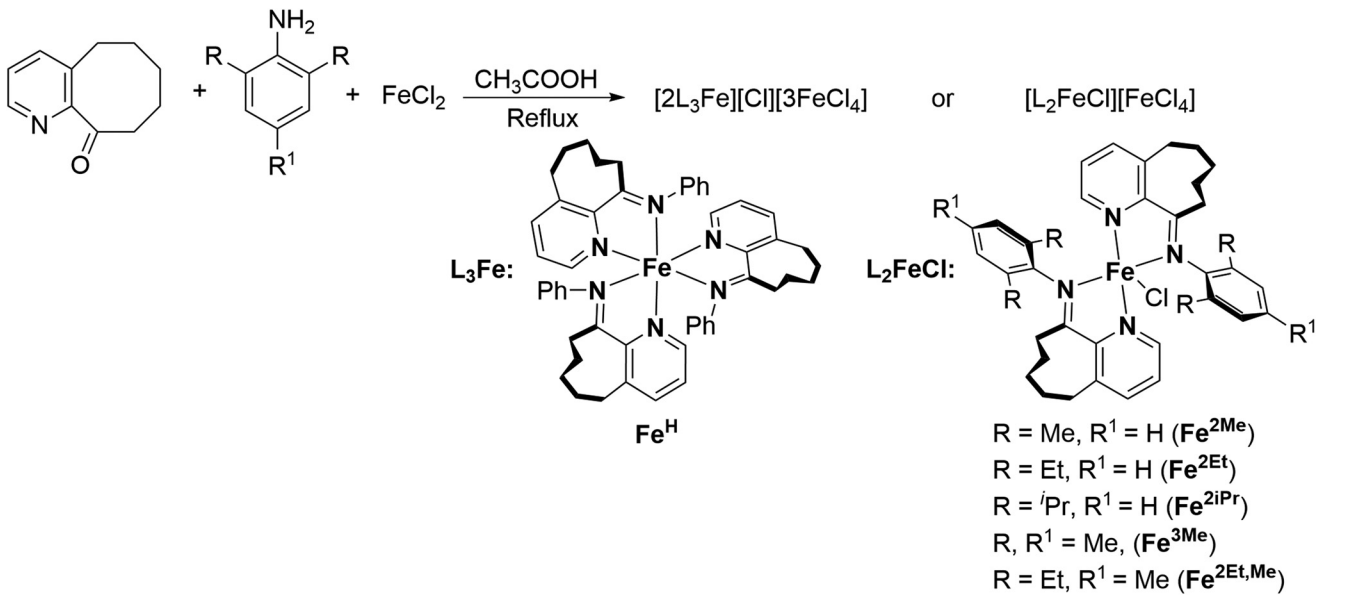

Scheme 1 One-pot synthesis of Fe complexes using acetic acid as solvent at boiling temperature.

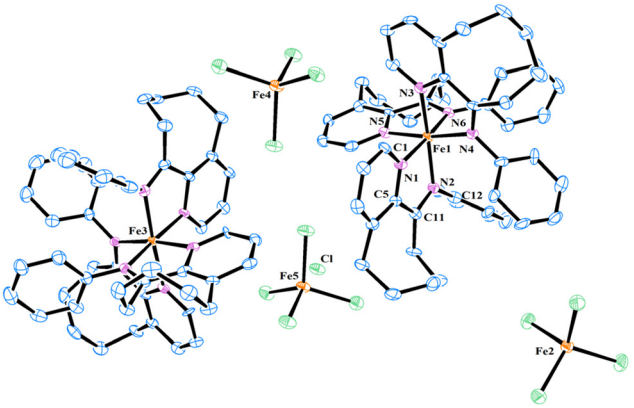

Fig. 2 Molecular structure of Fe^{H} with thermal ellipsoids shown at a 30% probability level. All hydrogen atoms are omitted for clarity. The iron center (Fe2) exhibited disorder, which is omitted for clarity. Selected bond lengths (Å): Fe1–N1 1.969(7), Fe1–N2 1.991(6), Fe1–N3 1.969(7), Fe1–N4 1.991(6), Fe1–N5 1.969(7), Fe1–N6 1.991(6), N1–C1 1.368(10), N1–C5 1.365(11), N2–C11 1.280(11), and N2–C12 1.440(9) and bond angles (°): N1–Fe1–N2 78.9(3), N3–Fe1–N4 78.9(3), N5–Fe1–N6 78.9(3), N1–Fe1–N4 89.7(3), N2–Fe1–N5 89.7(3), N3–Fe1–N6 89.7(3), N2–Fe1–N4 98.5(3), N2–Fe1–N6, 98.5(3), N4–Fe1–N6, 98.5(3), N2–Fe1–N3, 171.7(3), N4–Fe1–N5, 171.7(3), and N1–Fe1–N6, 171.7(3).

while the iron tetrachloride counterion adopts a typical tetrahedral geometry with characteristic bond lengths and angles. The bond distance between $N_{pyridine}$ and Fe is slightly shorter than the corresponding Fe–N_{imine} bond distance [Fe1–N1 = 1.969(7) Å *vs.* Fe1–N2 = 1.991(6) Å], indicating a stronger coordination of $N_{pyridine}$ compared to N_{imine} with the metal center. A similar discrepancy in the bond lengths is observed for other ligands chelated with the metal center. The bite angles N1–Fe1–N2, N3–Fe1–N4, and N5–Fe1–N6 all measure 78.9°, which are significantly smaller than other corresponding angles.[23] Moreover, the *N*-phenyl ring in the ligand framework is oriented almost perpendicularly to the chelate ring plane.

In contrast to the Fe^{H} cation, the coordination spheres of Fe^{2Me} and $Fe^{2Et,Me}$ cations adopt a geometry which can be best described as distorted trigonal bipyramidal around the iron center, characterized by bond lengths and angles typically found in bidentate iron complexes used for olefin polymerization. In the molecular structure of Fe^{2Me}, Cl1 and nitrogen atoms from the imine functionality (N2, N4) form a basal plane around the iron center with angles approximately close to 120° [N2–Fe1–Cl1 (119.4), N4–Fe1–Cl1 (120.8) and N2–Fe1–N4 (119.8)], while the N1 and N3 atoms occupy the axial positions of this basal plane with moderate distortion from 180°. Moreover, the *N*-aryl rings in the ligand framework are oriented almost perpendicularly to the plane of the chelate ring. The N1–Fe1–N2 and N3–Fe1–N4 bite angles are similar [73.68° and 73.86°, respectively], but are considerably smaller than the other four angles in the chelate ring. There are modest variations in the bond lengths. The bond distance between N_{imine} and the iron metal is slightly smaller than that of $N_{pyridine}$ and the metal bond distance [Fe1–N2 = 2.125(3) Å *vs.* Fe1–N1 = 2.182(3) Å], indicating a stronger coordination of N_{imine} compared to $N_{pyridine}$ with the metal center. Similar structural features are noticed for $Fe^{2Et,Me}$ and also consistent with the previous reports.[15,18,22a,23]

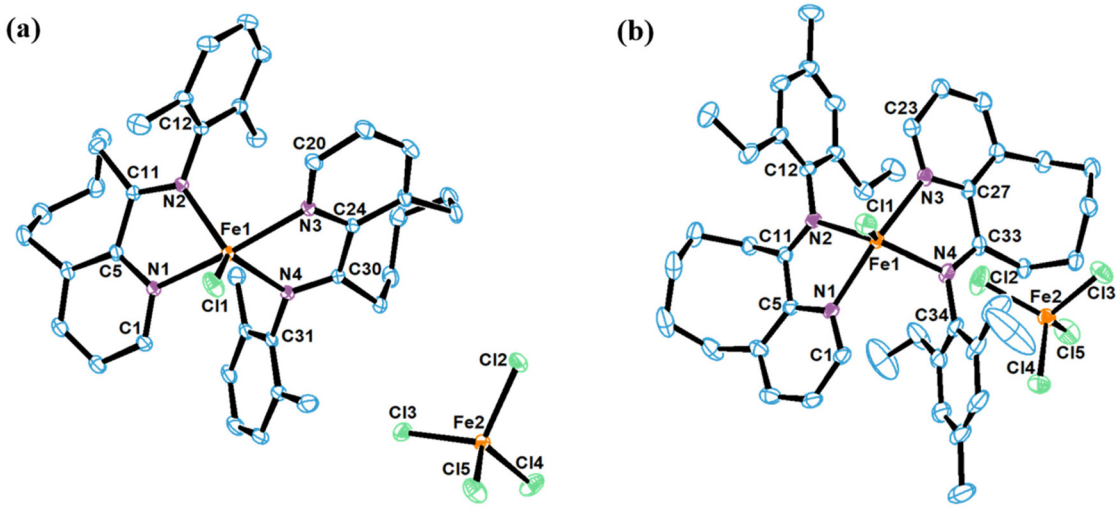

Fig. 3 Molecular structure of Fe^{2Me} (a) and $Fe^{2Et,Me}$ (b) with thermal ellipsoids shown at a 30% probability level. All hydrogen atoms are omitted for clarity. Ethyl groups of $Fe^{2Et,Me}$ exhibited disorder, which are omitted for clarity. Selected bond lengths (Å) for Fe^{2Me}: Fe1–N1 2.182(3), Fe1–N2 2.125(3), Fe1–N3 2.183(3), Fe1–N4 2.126(3), Fe1–Cl1 2.2574(10), N1–C1 1.332(4), N1–C5 1.354(4), N2–C11 1.285(4), and N2–C12 1.446(4) and bond angles (°): N2–Fe1–Cl1 119.36(8), N2–Fe1–N4 119.85(10), N4–Fe1–Cl1 120.78(8), N1–Fe1–Cl1 98.85(8), N3–Fe1–Cl1 98.13(8), N1–Fe1–N2 73.68(10), N3–Fe1–N4 73.86(10), and N1–Fe1–N3 163.01(10). Selected bond lengths (Å) for $Fe^{2Et,Me}$: Fe1–N1 2.193(3), Fe1–N2 2.141(3), Fe1–N3 2.183(3), Fe1–N4 2.140(3), Fe1–Cl1 2.2536(10), N1–C1 1.335(4), N1–C5 1.352(4), N2–C11 1.287(4), and N2–C12 1.442(4) and bond angles (°): N2–Fe1–Cl1 116.05(8), N2–Fe1–N4 124.95(11), N4–Fe1–Cl1 119.00(9), N1–Fe1–Cl1 101.90(8), N3–Fe1–Cl1 103.83(8), N1–Fe1–N2 72.97(10), N3–Fe1–N4 72.83(11), and N1–Fe1–N3 154.27(11).

Isoprene polymerization

Optimization of reaction conditions. Previous studies have shown that apart from the precatalyst structure, the choice of cocatalyst and reaction conditions significantly influence isoprene polymerization and the resulting polymer microstructure.[8a,12f,16,24] Therefore, we initiated our investigation by evaluating three different aluminium compounds ($AlMe_2Cl$, $AlEt_2Cl$, and MAO) as potential cocatalysts for isoprene polymerization using complex **Fe^{H}** (Table 1, entries 1–3). Surprisingly, $AlMe_2Cl$ and $AlEt_2Cl$ were ineffective in activating the complex, while MAO, with an Al/Fe ratio of 100, achieved complete monomer conversion at an Ip/Fe ratio of 4000 (Table 1, entry 3). Thus, MAO was selected as the preferred cocatalyst for further exploration of isoprene polymerization. Subsequently, a systematic investigation was carried out with **Fe^{H}** as the precatalyst in conjunction with MAO, under various reaction conditions including the cocatalyst amount (Al/Fe ratio = 100, 40 or 20), reaction temperature (T = −20, 0, 25, 40, 60, 80 or 100 °C) and reaction time (t = 60, 45, 30, 15, 5 or 2 min). The resulting polyisoprenes were characterized by GPC, and ^{1}H and ^{13}C NMR spectra. The polymerization results are given in Tables 2 and 3.

Besides the cocatalyst nature, activity and molecular weights also relied on the changes in the cocatalyst amount employed. Monomer conversion and polymerization activity decreased as the Al/Fe ratio reduced from 100. Despite this decline, the activity remained notably high, even at a very low Al/Fe ratio of 20, yielding an 86% conversion with an activity of 2.36×10^5 g_{PI} $(mol_{Fe}, h)^{-1}$. Remarkably, the complex **Fe^{H}** achieved full monomer conversion with the highest activity of 2.74×10^5 g_{PI} $(mol_{Fe}, h)^{-1}$ at an Al/Fe ratio of 100 (Table 2, entry 1).[12a,17,18,24] It is noteworthy that polymer molecular weights exhibited minimal variation at Al/Fe ratios of 100 or 40, suggesting negligible occurrence of chain transfer reactions to aluminium species at these cocatalyst amounts. This phenomenon is further reflected by the narrow polymer molecular weight distributions. In contrast, changing the Al/Fe ratio from 20 to 40 resulted in an increase in polymer molecular weight from 3.0×10^5 g mol^{-1} to 3.88×10^5 g mol^{-1}.[2d,12e] Likely, chain propagation reactions were more rapid compared to chain transfer reactions, given the enhanced monomer conversion resulting from an increase in the quantity of the cocatalyst. Regarding the microstructure of the polymer, there is no significant effect of variations in the cocatalyst amount on the mode of the monomer coordination–insertion reaction as the

Table 1 Selection of cocatalyst for activating the **Fe^{H}** complex towards polymerization of isoprene[a]

						Microstructure[e] (mol%)		
Entry	Cocat.	Con.[b] (%)	Act.[c]	M_n[d] (g mol^{-1})	$Đ$[d]	*cis*-1,4	*trans*-1,4	1,4/3,4
1	$AlMe_2Cl$	Trace	—	—	—	—	—	—
2	$AlEt_2Cl$	Trace	—	—	—	—	—	—
4	MAO	>99	2.74	3.62	2.23	>51	<1	52/48

[a] General conditions: **Fe^{H}** amount: 5 μmol, isoprene (Ip): 20 mmol, Ip/Fe: 4000, toluene: 5 mL, cocatalyst: MAO, Al/Fe ratio: 100, reaction temperature: 25 °C, reaction time: 1 h. [b] Isolated yield. [c] 10^5 g_{PI} $(mol_{Fe}, h)^{-1}$. [d] M_n: 10^5 g mol^{-1}; determined by GPC. [e] Determined by ^{1}H and ^{13}C NMR spectra.

Table 2 Selection of the cocatalyst amount, reaction temperature and run time[a]

								Microstructure[e] (mol%)		
Entry	Al/Fe	Temp. (°C)	Time (min)	Conv.[b] (%)	Act.[c]	M_n[d] (10^5)	$Đ$[d]	*cis*-1,4	*trans*-1,4	1,4/3,4
1	100	25	60	>99	2.74	3.62	2.23	>51	<1	52/48
2	40	25	60	95	2.60	3.88	2.16	>49	<1	50/50
3	20	25	60	86	2.36	3.00	1.97	>48	<1	49/51
4	100	−20	60	69	1.90	2.01	2.07	>8	<1	09/91
5	100	0	60	95	2.60	2.28	2.29	>14	<1	15/85
6	100	40	60	>99	2.74	2.71	2.07	>50	<1	51/49
7	100	60	60	96	2.64	2.15	2.60	>51	<1	52/48
8	100	80	60	82	2.24	1.97	2.94	>51	<1	52/48
9	100	100	60	66	1.80	0.78	3.67	50	4	54/46
10	100	25	45	>99	3.66	2.92	2.55	>51	<1	52/48
11	100	25	30	>99	5.48	2.62	3.19	>50	<1	51/49
12	100	25	15	87	9.52	2.46	2.90	>49	<1	50/50
13	100	25	5	69	23.8	2.33	2.22	>49	<1	50/50
14	100	25	2	48	39.6	2.19	2.57	>48	<1	49/51

[a] General conditions: **Fe^{H}** amount: 5 μmol, isoprene (Ip): 20 mmol, MAO, Ip/Fe: 4000, toluene: 5 mL. [b] Isolated yield. [c] 10^5 g^{PI} $(mol_{Fe}, h)^{-1}$. [d] M_n: 10^5 g mol^{-1}; determined by GPC. [e] Determined by ^{1}H and ^{13}C NMR spectra.

Table 3 Polymerization of isoprene by using different Fe complexes[a]

Entry	Cat.	Conv.[b] (%)	Act.[c]	M_n [d]	$Đ$[d]	Microsctructures[e] (mol%)		
						cis-1,4	*trans*-1,4	1,4/3,4
1	$\mathbf{Fe^{H}}$	>99	5.48	2.67	3.22	>50	<1	51/49
2	$\mathbf{Fe^{2Me}}$	72	3.92	1.39	3.57	>57	<1	58/42
3	$\mathbf{Fe^{2Et}}$	61	3.36	0.45	2.19	55	5	60/40
4	$\mathbf{Fe^{2iPr}}$	50	2.76	0.37	3.20	55	8	63/37
5	$\mathbf{Fe^{3Me}}$	70	3.84	0.88	2.61	51	14	65/35
6	$\mathbf{Fe^{2Et,Me}}$	58	3.20	0.43	4.28	48	21	69/31

[a] General conditions: iron precatalyst amount: 5 μmol, isoprene (Ip): 20 mmol, Ip/Fe: 4000, toluene: 5 mL, cocatalyst: MAO, Al/Fe ratio: 100, temperature: 25 °C, time: 30 min. [b] Isolated yield. [c] 10^5 g_{PI} $(mol_{Fe}, h)^{-1}$. [d] M_n: 10^5 g mol^{-1}; determined by GPC. [e] Determined by ^1H and ^{13}C NMR spectra.

resultant polyisoprene contained almost equal proportions of *cis*-1,4 and 3,4 units, in the range of 48–51% and 49–52%, respectively. Notably, similar observations have been reported previously in the literature.[2d,25]

As shown in Table 2, entries 1 and 4–9, the reaction temperature exerts a significant impact on monomer conversion, catalytic activity, and various polymer properties such as the molecular weight, dispersity, and microstructure. Gradually elevating the reaction temperature from −20 °C to 0 °C, 25 °C, and 40 °C resulted in a progressive improvement in both monomer conversion and activity. However, further increases in temperature resulted in a consistent decrease in yield and activity (Fig. 4a). Complete conversion with the highest activity of 2.74×10^5 g_{PI} $(mol_{Fe}, h)^{-1}$ was achieved at 25 °C or 40 °C. At 80 °C and 100 °C, comparatively lower activity levels of 2.24×10^5 g_{PI} $(mol_{Fe}, h)^{-1}$ and 1.8×10^5 g_{PI} $(mol_{Fe}, h)^{-1}$ were obtained, indicating partial decomposition of active species. Despite the gradual decrease in activity with increasing reaction temperature, the $\mathbf{Fe^{H}}$/MAO system still exhibited good activity at elevated temperatures, demonstrating high thermal stability of the active species.[9] As shown in Fig. 4b, polymer molecular weights showed a gradual decrease with rising reaction temperature. The highest polymer molecular weight of 3.62×10^5 g mol^{-1} was observed at 25 °C, which gradually declined to 0.78×10^5 g mol^{-1} at 100 °C. This suggests that higher temperatures facilitate chain transfer reactions relative to chain propagation, resulting in reduced polymer molecular weights.[8c,12a,25] The dispersity of polymer molecular weights became relatively broad when the temperature increased from 60 °C to 100 °C ($Đ$ = 2.60–3.67), also indicating partial decomposition of active species at higher temperatures. Furthermore, variations in the reaction temperature significantly influenced the regioselectivity of monomer addition in the polymer chain. Lower temperatures favored 3,4 addition; for instance, polymerization at −20 °C resulted in 91% regioselectivity for 3,4 addition, decreasing to 85% at 0 °C and further to 48% at 20 °C (Table 2, entries 1, 4 and 5). However, increasing the temperature beyond this range had a negligible impact on regioselectivity. Additionally, across the temperature range (−20 to 100 °C), the stereoselectivity remained largely consistent, favoring *cis*-1,4 addition over *trans*-1,4 addition. This observation suggests that higher temperature induced rotations of the *N*-aryl unit could alter the steric environment around the active species, potentially modifying the coordination mode of monomer insertion from 3,4 to *trans*-1,4.[25b,c]

The catalytic performance of $\mathbf{Fe^{H}}$/MAO was further explored at shorter reaction run times such as 45, 30, 15, 5, or 2 minutes, while maintaining a constant temperature of 25 °C

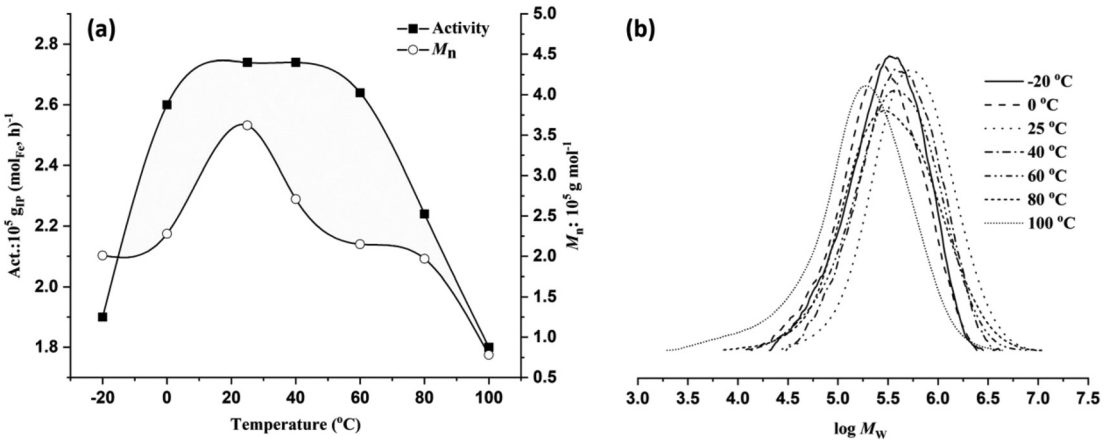

Fig. 4 Activity and M_n *versus* temperature (a) and GPC curves at different reaction temperatures (b).

(Table 2, entries 10–14). This investigation aimed to determine the minimum time required to achieve complete monomer conversion. Apparently, complete conversion was attained within 30 min, but as the reaction time decreased beyond that point, the conversion gradually decreased (87%, 69%, and 48% for 15, 5, and 2 min, respectively), revealing that optimal run time of 30 min was necessary to achieve full conversion for an Ip/Fe ratio of 4000. The calculated polymerization activity increased as the reaction time was decreased, reaching a maximum activity of 3.96×10^6 g_{PI} $(mol_{Fe}, h)^{-1}$ with a 2 min reaction time, highlighting a short incubation period for the cocatalyst to activate **Fe^{H}**.[18,26] The number-average molecular weights of polyisoprene exhibited a gradual increase with extended reaction times but exhibited a significant deviation from linear behavior after 30 minutes. The dispersity remained narrow across different reaction times ($Đ$ = 2.22–3.19).[18,26] There was no significant change in the selectivity of monomer insertion at varying reaction times, with nearly equal proportions of 1,4 and 3,4 monomer additions (1,4/3,4 ≈ 50/50). The ^{1}H and ^{13}C NMR spectra of representative polyisoprene obtained over a run time of 30 min are presented in Fig. 5. Furthermore, there was a strong preference for *cis*-1,4 structures over *trans*-1,4 structures in the resulting polyisoprenes.[18]

Ligand effect on isoprene polymerization. The impact of the ligand structure in iron complexes (**Fe^{2Me}**, **Fe^{2Et}**, **Fe^{2iPr}**, **Fe^{3Me}**, **Fe^{2Et,Me}**) on their catalytic performance in isoprene polymerization was investigated under optimal conditions established by **Fe^{H}**/MAO [Al/Fe ratio = 100, temperature = 25 °C, time = 30 min]. According to the polymerization data presented in Table 3, the nature of the R substituent of the aniline significantly influenced the catalytic performance, including monomer conversion, activity, and polymer properties like molecular weights, dispersity, and selectivity. As depicted in Fig. 6a, all iron precatalysts displayed high activities, ranging from 2.76×10^5 g_{PI} $(mol_{Fe}, h)^{-1}$ to 5.48×10^5 g_{PI} $(mol_{Fe}, h)^{-1}$, and activity with respect to the ligand structure follows the order **Fe^{H}** > **Fe^{2Me}** (R = Me) ≈ **Fe^{3Me}** (R, R^1 = Me) > **Fe^{2Et}** (R = Et) ≈ **Fe^{2Et,Me}** (R, = Et, R1 = Me) > **Fe^{2iPr}** (R = iPr). It is evident that increasing steric hindrance of the R substituents of the aniline leads to decreased polymerization activities and monomer conversions, likely due to hindered monomer coordination with the metal center. For example, **Fe^{H}**, with no substituent on the aniline, displayed the maximum activity of 5.48×10^5 g_{PI} $(mol_{Fe}, h)^{-1}$ with complete conversion, while **Fe^{2Me}**, **Fe^{2Et}**, and **Fe^{2iPr}** bearing dialkyl-substituted anilines, exhibited lower polymerization activity and incomplete monomer conversion in the fixed reaction time. Among these Fe precatalysts, **Fe^{2iPr}** featuring the bulkiest steric substituent was the least active precatalyst.

Additionally, the electron-donating effect of the R^1 substituent at the *para* position of the aniline resulted in a slight decline in monomer conversion and activity. This decrease can be attributed to the electron-donating nature of R^1, which decreased the Lewis acidic character of the metal and, in turn, reduced its ability to coordinate with the monomer. Consequently, **Fe^{3Me}** and **Fe^{2Et,Me}** displayed lower polymerization activity compared to their analogue complexes, **Fe^{2Me}** and **Fe^{2Et}**.[2d,12a] The rate of polymerization, which depends on the ligand structure, reveals that the cations of these iron complexes, after reacting with MAO, yield active species with single-site behaviour, as reflected in the narrow and unimodal molecular weight distributions of the resulting polymer. On the other hand, it is likely that the iron center of the anion, after reacting with MAO, remains inactive or intact during the initiation of polymerization.

With regard to the molecular weight of the resulting polymer, the steric hindrance induced by the R substituent of

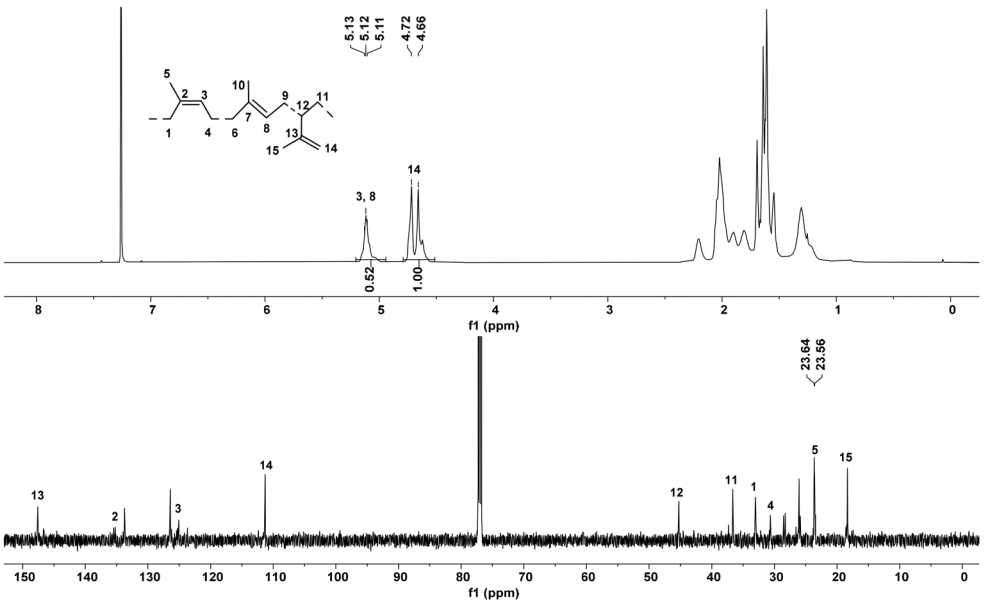

Fig. 5 ^{1}H and ^{13}C NMR spectra of the representative sample of polyisoprene obtained using the **Fe^{H}**/MAO system (Table 2, entry 11).

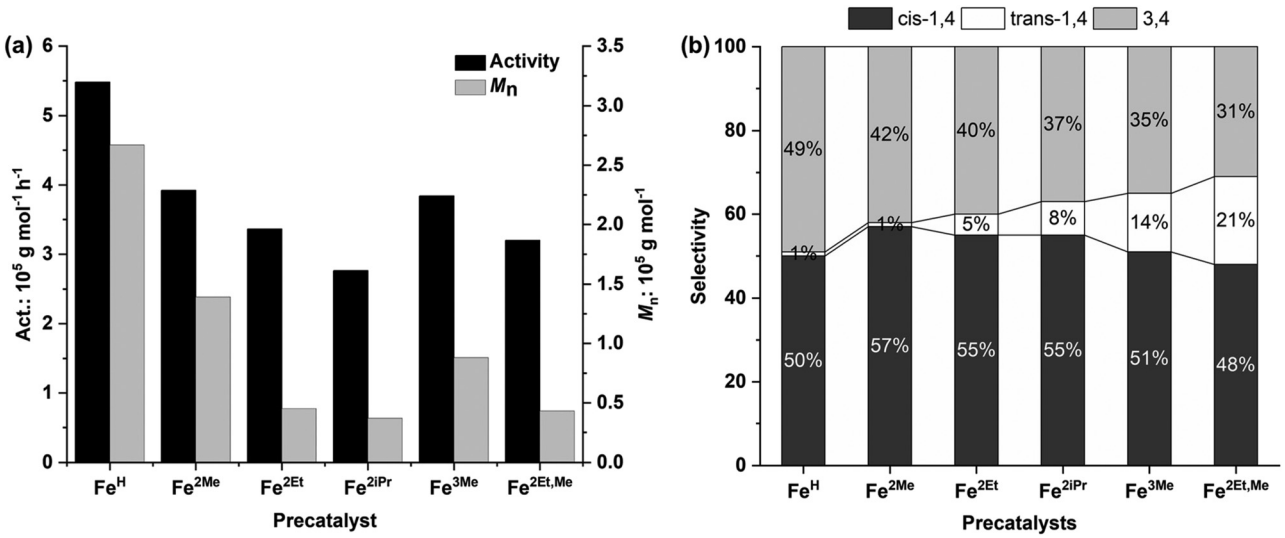

Fig. 6 Polymerization activity and number average molecular weight (a) and selectivity (b) *versus* the structure of precatalysts.

the aniline leads to a reduction in the molecular weights of the resulting polyisoprenes (Fig. 6a). **Fe^{H}** without steric hindrance at the *ortho* position of aniline produced a polyisoprene with the highest molecular weight, up to 2.67×10^5 g mol^{-1}. **Fe^{2Me}** with lower steric hindrance yielded a polyisoprene with the second highest molecular weight, while **Fe^{2iPr}**, with significant steric hindrance resulted in a polyisoprene with the lowest molecular weight. These findings suggest that large steric groups hinder monomer coordination–insertion, leading to more pronounced chain transfer/termination reactions. The dispersity of polymer molecular weights ranged from unimodal to broad ($Đ$ = 2.19–4.28), mainly depending on the steric hindrance of the R substituents of the aniline.[12g,18]

The influence of the precatalyst structure on polymerization selectivity was also observed. According to the results from ^{1}H and ^{13}C NMR spectra (Fig. 5 and 7, S14–S17†), the prepared Fe complexes exhibited a preference for 1,4 additions over 3,4 additions, in the range of 51–69%, (Fig. 6b), primarily influenced by the steric hindrance of the R substituent in the precatalyst structure (Table 3, entries 1–6). The increase in steric hindrance induced by the *ortho* substituents promotes 1,4 additions. Specifically, this rise in 1,4 units corresponds to an

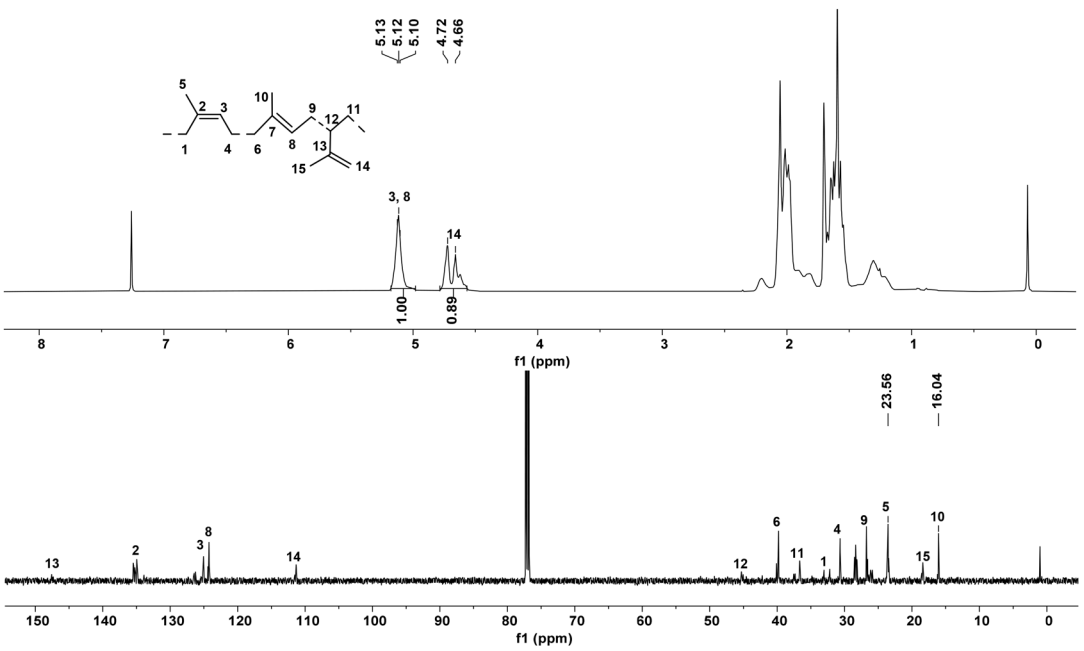

Fig. 7 ^{1}H and ^{13}C NMR spectra of the representative sample of polyisoprene obtained using the **Fe^{2Et,Me}**/MAO system (Table 3, entry 6).

Table 4 Impact of reducing precatalyst loading on isoprene polymerization using Fe^{H} as representative precatalyst[a]

Entry	Ip/Fe	Con.[b] (%)	Act.[c]	M_n [d] (g mol^{-1})	$Đ$[d]	Microstructure[e] (mol%)		
						cis-1,4	*trans*-1,4	1,4/3,4
1	4000	>99	5.48	2.62	3.19	>50	<1	51/49
2	8000	95	10.4	2.67	3.22	>50	<1	51/49
3	16 000	89	19.5	2.36	1.95	>49	<1	50/50
4	20 000	87	24.0	2.71	1.69	>49	<1	50/50
5	40 000	73	40.0	2.63	1.53	>49	<1	50/50

[a] General conditions: precatalyst: Fe^{H}, isoprene (Ip): 20 mmol, toluene: 5 mL, cocatalyst: MAO, Al/Fe ratio: 100, temperature: 25 °C, time: 30 min. [b] Isolated yield. [c] 10^5 g_{PI} (mol_{Fe}, h)$^{-1}$. [d] M_n: 10^5 g mol^{-1}; determined by GPC. [e] Determined by ^{1}H and ^{13}C NMR spectra.

increase in the *trans*-1,4/*cis*-1,4 ratio, contrasting with the sterically less bulky Fe^{H} complex, which produces nearly no *trans*-1,4 units. Thus, polyisoprenes derived from $Fe^{2Et,Me}$ exhibited a regioselectivity of up to 69% for 1,4 addition, including 21% *trans*-1,4 units.[12g,15,19] In summary, these catalytic systems tend to polymerize isoprene with high polymerization activity, high polymer molecular weights, moderate regioselectivity, and high stereoselectivity.

Impact of reducing precatalyst loading on isoprene polymerization

Fe^{H}, at a concentration of 5 μmol, exhibited high polymerization activity, achieving complete monomer conversion within 30 min for an Ip/Fe ratio of 4000. To explore the impact of precatalyst quantity on isoprene polymerization, polymerization tests were conducted using reduced amounts of precatalyst, while maintaining a fixed quantity of MAO and isoprene (2 mL) at room temperature. As shown in Table 4, polymerization activity increased as the catalyst amount was decreased. Despite the decrease in conversions, high to excellent conversions were still achieved, along with high polymerization activities. Remarkably, even at a precatalyst loading of 0.0025 mol%, which is 20 times lower than the initially used catalyst loading (5 μmol), polymerization proceeded smoothly with a conversion of 73% and an excellent activity of 4.0×10^6 g_{PI} (mol_{Fe}, h)$^{-1}$, highlighting promising efficiency of the iron catalyst for isoprene polymerization.[9] The decrease in the catalyst loading demonstrated negligible impact on polymer molecular weights, with only a slight improvement observed, reaching up to 2.71×10^5 g mol^{-1}. This is likely due to the gradual reduction in monomer conversion. On the other hand, the dispersity gradually decreased to a narrow value of 1.53 (Table 4, entry 5).[12g] There was no significant impact of precatalyst quantity on selectivity, with similar monomer additions (*cis*-1,4/3,4: 1/1) observed at different precatalyst amounts (Table 4).

Comparison with previously reported iron complexes

In the class of iminopyridine Fe and Co precatalysts investigated for isoprene polymerization, Fe precatalysts bearing *N*-octyl or *N*-aryl imine groups were particularly effective in controlling the selectivity of monomer additions. The resulting polyisoprene displayed 1,4 and 3,4 structures in the range of 2 : 1 to 12 : 1, with complete *cis* or *trans* selectivity for 1,4 structures (**C** and **D**, Fig. 1).[14] The alkyl and disubstituted aryl variants of these Fe precatalysts exhibited similar catalytic performance in terms of activity (up to 8.3×10^4 g_{PI} (mol_{Fe}, h)$^{-1}$ and polymer properties. The aminopyridine iron analogues (**E**, Fig. 1) also exhibited high activities, reaching up to 1.9×10^6 g_{PI} (mol_{Fe}, h)$^{-1}$ with a significant preference for 3,4 enchainment (approximately 50%).[12e] The incorporation of a methyl group at the imine carbon in these Fe precatalysts had a significant positive effect on improving activity (up to 2.0×10^7 g_{PI} (mol_{Fe}, h)$^{-1}$) along with high monomer stereoselectivity (*cis*-1,4/*trans*-1,4 = 100) (**F** and **G**, Fig. 1).[8d,16,18] Cyclohexyl-fused iminopyridine Fe precatalysts further enhanced polymerization activity, reaching a peak of 1.0×10^8 g_{PI} (mol_{Fe}, h)$^{-1}$, while maintaining high thermal stability and tunable 1,4-*cis*/*trans* stereoslectivity from <1/99 to 96/4 (**H**, Fig. 1).[19] These iron catalysts with larger carbocyclic rings, such as cycloheptyl (**I**, Fig. 1) exhibited even higher activity, reaching 1.2×10^8 g_{PI} (mol_{Fe}, h)$^{-1}$, and produced polyisoprenes with consistently high molecular weights.[20] Similarly, the title Fe complexes bearing a fused cyclooctyl ring were highly active, providing activity in the level of 10^5 to 10^6 g_{PI} (mol_{Fe}, h)$^{-1}$ with the use of very small amounts of precatalyst and cocatalyst (**J**, Fig. 1). The resulting polyisoprene was mainly composed of *cis*-1,4 structures along with a variable amount of 3,4 units in the range of 31–49%. Moreover, the confinement of the iminopyridine ligand framework with the incorporation of the cyclooctyl ring also improved thermal stability, enabling smooth polymerization at elevated temperatures (up to 100 °C). In comparison to iminopyridine cobalt precatalysts, the prepared iron complexes exhibited significantly higher polymerization activity and produced high molecular weight polyisoprenes. Overall, the prepared iron complexes proved to be highly active precatalysts for the synthesis of high molecular weight polyisoprenes.

Experimental section

Synthesis and characterization of Fe complexes

General procedure (taking Fe^{H} as an example). A suspension of 5,6,7,8,9-pentahydrocycloocta[*b*]pyridin-10-one (100 mg, 0.57 mmol), $FeCl_2$ (72 mg, 0.57 mmol) and aniline (93 mg, 0.68 mmol) in acetic acid (8 ml) was refluxed for half day with constant magnetic stirring. Subsequently, the reaction mixture

was cooled down and diethyl ether was added for precipitation. Following workup with filtration, washing with diethyl ether thrice and drying, $\mathbf{Fe^{H}}$ was afforded as purple powder in good yield (58% yield). FT-IR (cm^{-1}): 3445 (m), 3062 (m), 2929 (s), 2857 (s) 1635 (s), 1585 (s), 1558 (w), 1485 (s), 1448 (m), 1347 (m), 1331 (s), 1266 (s), 1248 (m), 1214 (m) 1178 (s), 1101 (m), 1002 (m), 871 (w), 796 (s), 752 (s), 727 (m), 701 (s). Anal. calcd for $[2C_{51}H_{54}FeN_6][Cl][3FeCl_4][4C_6H_{14}][4MeCN]$: C, 58.50; H, 6.45; N, 8.15. Found: C, 58.67; H, 5.70; N, 8.26.

Synthesis of Fe^{2Me}. Under similar conditions, the amount of corresponding reactants and the procedure adopted for $\mathbf{Fe^{H}}$, $\mathbf{Fe^{2Me}}$ was obtained as a reddish brown solid (49% yield). FT-IR (cm^{-1}): 3418 (s), 3070 (w), 2932 (s), 2862 (m), 1621 (m), 1600 (s), 1567 (s), 1491 (w), 1449 (s), 1346.00 (m), 1332 (m), 1274 (s), 1248 (m), 1202 (s), 1182 (w), 1127 (m), 1102 (m), 903 (m), 862 (m), 800 (m), 774 (s), 676 (m). Anal. calcd for $[C_{38}H_{44}ClFeN_4][FeCl_4]$: C, 53.97; H, 5.24; N, 6.62. Found: C, 53.86; H, 5.18; N, 6.67.

Synthesis of Fe^{2Et}. Under similar conditions, the amount of corresponding reactants and the procedure adopted for $\mathbf{Fe^{H}}$, $\mathbf{Fe^{2Et}}$ was obtained as a maroon solid (47% yield). FT-IR (cm^{-1}): 3413 (m), 3068 (m), 2969 (m), 2933 (s), 2862 (m), 1629 (m), 1598 (s), 1567 (ss), 1492 (m), 1448 (s), 1346 (m), 1330 (m), 1271 (s), 1248 (m), 1194 (s), 1127 (m), 1112 (w), 1091 (w), 906 (m), 864 (m), 794 (s), 677 (m). Anal. calcd for $[C_{42}H_{52}ClFeN_4][FeCl_4]$: C, 55.94; H, 5.81; N, 6.21. Found: C, 55.89; H, 5.79; N, 6.39.

Synthesis of Fe^{2iPr}. Under similar conditions, the amount of corresponding reactants and the procedure adopted for $\mathbf{Fe^{H}}$, $\mathbf{Fe^{2iPr}}$ was obtained as a green solid (31% yield). FT-IR (cm^{-1}): 3370 (m), 3084 (m), 2932 (s), 2861 (m), 1633 (s), 1584 (m), 1485 (w), 1454 (s), 1348 (m), 1330 (m), 1267 (m), 1245 (m), 1176 (m), 1161 (s), 1125 (m), 1097 (m), 806 (m), 710 (w), 686 (m). Anal. calcd for $[C_{46}H_{60}ClFeN_4][FeCl_4]$: C, 57.68; H, 6.31; N, 5.85. Found: C, 57.72; H, 6.24; N, 5.78.

Synthesis of Fe^{3Me}. Under similar conditions, the amount of corresponding reactants and the procedure adopted for $\mathbf{Fe^{H}}$, $\mathbf{Fe^{3Me}}$ was obtained as a green solid (40% yield). FT-IR (cm^{-1}): 3367 (w), 2930 (s), 2860 (m), 1632 (s), 1584 (m), 1520 (w), 1485 (s), 1453 (s), 1348 (m), 1330 (m), 1267 (m), 1245 (m), 1161 (s), 1125 (w), 1097 (m), 1039 (m), 1036 (w), 855 (s), 805 (s), 704 (m), 686 (s). Anal. calcd for $[C_{40}H_{48}ClFeN_4][FeCl_4]$: C, 54.98; H, 5.54; N, 6.41. Found: C, 54.91; H, 5.66; N, 6.48.

Synthesis of $Fe^{2Et,Me}$. Under similar conditions, the amount of corresponding reactants and the procedure adopted for $\mathbf{Fe^{H}}$, $\mathbf{Fe^{2Et,Me}}$ was obtained as a green solid (37% yield). FT-IR (cm^{-1}): 3445 (s), 2930 (s), 2859 (s), 1634 (s), 1584 (s), 1521 (w), 1486 (s), 1454 (s), 1347 (m), 1330 (m), 1267 (m), 1245 (m), 1161 (s), 1125 (w), 1096 (m), 854 (s), 805 (s), 704 (m), 686 (s). Anal. calcd for $[C_{44}H_{56}ClFeN_4][FeCl_4]$: C, 56.83; H, 6.07; N, 6.03. Found: C, 56.87; H, 6.11; N, 6.01.

Conclusion

In summary, a novel series of iron complexes in the form of ion pairs $[2L_3Fe][Cl][3FeCl_4]$ and $[L_2FeCl][FeCl_4]$ was efficiently prepared using a simple, cost-effective, one-pot method and comprehensively characterized through various analytical techniques, including FTIR, elemental composition, and single crystal X-ray diffraction. Upon activation with methylaluminoxane, these iron complexes not only exhibited high activity but also generated high molecular weight polyisoprenes. Systematic variations in the steric hindrance of *ortho*-substituents on the ligands revealed that bulkier groups had a detrimental effect on the polymerization activity and polymer molecular weight. The precatalyst with the least steric hindrance displayed the highest activity, achieving 2.74×10^5 g_{PI} $(mol_{Fe}, h)^{-1}$ and complete conversion of 4000 equiv. of monomer in just 30 min. Even at a very low precatalyst loading of 0.0025 mol%, polymerization proceeded smoothly with a remarkable activity of 4.0×10^6 g_{PI} $(mol_{Fe}, h)^{-1}$ and high polymer molecular weights (M_n = 2.63×10^5 g mol^{-1}). The impact of reaction temperature, time, and cocatalyst amount was systematically explored, revealing that $\mathbf{Fe^{H}}$-MAO displayed high thermal stability and consistently yielded high polymer molecular weights over a wide temperature range (−20–100 °C). All resulting polyisoprenes exhibited mixed *cis*-1,4/3,4 microstructures, which were significantly influenced by the ligand structure and polymerization temperature. Polymerization at lower temperatures favored 3,4 additions (up to 91%), while more sterically hindered iron precatalysts produced polyisoprenes with *cis*-1,4 selectivity.

Conflicts of interest

There are no conflicts to declare.

Acknowledgements

This work has been financially supported by the Chemistry and Chemical Engineering Guangdong Laboratory (2111018 and 2132012), and Q. M. would like to express gratitude towards the Foreign Youth Talent Program (QN2022030008L) for their support. N. Y. would like to express gratitude towards the Chinese Government Scholarship-Belt and Road Program and the ANSO Scholarship Program for their support.

References

1 (*a*) G. Ricci, A. Sommazzi, F. Masi, M. Ricci, A. Boglia and G. Leone, *Coord. Chem. Rev.*, 2010, **254**, 661–676; (*b*) G. Ricci, G. Pampaloni, A. Sommazzi and F. Masi, *Macromolecules*, 2021, **54**, 5879–5914.

2 (*a*) Y. Champouret, O. H. Hashmi and M. Visseaux, *Coord. Chem. Rev.*, 2019, **390**, 127–170; (*b*) H. Wang, Y. Yang, M. Nishiura, Y. I. Hong, Y. Nishiyama, Y. Higaki and Z. Hou, *Angew. Chem., Int. Ed.*, 2022, **61**, e202210023; (*c*) M. Zhao, L. Wang, Q. Mahmood, C. Jing, G. Zhu, X. Zhang, X. Chen and Q. Wang, *J. Polym. Sci.*, 2020, **58**,

2708–2717; (*d*) N. Yousuf, Y. Ma, Q. Mahmood, W. Zhang, M. Liu, R. Yuan and W.-H. Sun, *Catalysts*, 2023, **13**, 1120.

3 (*a*) L. Zhang, Y. Luo and Z. Hou, *J. Am. Chem. Soc.*, 2005, **127**, 14562–14563; (*b*) L. Zhang, T. Suzuki, Y. Luo, M. Nishiura and Z. Hou, *Angew. Chem., Int. Ed.*, 2007, **46**, 1909–1913; (*c*) H. Liu, J. He, Z. Liu, Z. Lin, G. Du, S. Zhang and X. Li, *Macromolecules*, 2013, **46**(9), 3257–3265; (*d*) G. Zhang, B. Deng, S. Wang, Y. Wei, S. Zhou, X. Zhu, Z. Huang and X. Mu, *Dalton Trans.*, 2016, **45**, 15445; (*e*) Y. Ren, J. T. Miller, S. T. Polderman, T. D. Vo, A. C. M. Wallace, J. M. O. Cue, S. T. Tran, M. C. Biewer and M. C. Stefan, *RSC Adv.*, 2019, **9**, 3345.

4 S. K. De and J. R. White, *Rubber Technologists Handbookm*, Rapra Technology Limited, Shawbury, UK, 2001, pp. 49–51.

5 S. Ouardad, M.-E. Bakleh, S. V. Kostjuk, F. Ganachaud, J. E. Puskas, A. Deffieux and F. Peruch, *Polym. Int.*, 2012, **61**, 149–156.

6 (*a*) E. Shoenberg, H. A. Marsh, S. J. Walters and W. M. saltman, *Rubber Chem. Technol.*, 1979, **52**, 526–604; (*b*) C. W. Kamienski, *Ind. Eng. Chem.*, 1965, **57**, 38–55; (*c*) L. Friebe, O. Nuyken and W. Obrecht, *Adv. Polym. Sci.*, 2006, **204**, 1–154.

7 (*a*) J. S. Lasky, H. K. Garner and R. H. Ewart, *Ind. Eng. Chem. Prod. Res. Dev.*, 1962, **1**, 82–85; (*b*) M. Zhao, Q. Mahmood, C. Jing, L. Wang, G. Zhu, X. Zhang and Q. Wang, *Polymers*, 2019, **11**, 1122.

8 (*a*) A. He, G. Wang, W. Zhao, X. Jiang, W. Yao and W.-H. Sun, *Polym. Int.*, 2013, **62**, 1758–1766; (*b*) G. Wang, X. Jiang, W. Zhao, W.-H. Sun, W. Yao and A. He, *J. Appl. Polym. Sci.*, 2013, **131**, 1; (*c*) M. N. Alnajrani and F. S. Mair, *Dalton Trans.*, 2016, **45**, 10435–10446; (*d*) M. Scoti, F. D. Stefano, G. Zanchin, G. Leone, C. D. Rosa and G. Ricci, *Macromolecules*, 2023, **56**, 4629–4638.

9 L. Wang, X. Wang, H. Hou, G. Zhu, Z. Han, W. Yang, X. Chen and Q. Wang, *Chem. Commun.*, 2020, **56**, 8846–8849.

10 (*a*) H. Noguchi and S. Kambara, *J. Polym. Sci., Part B: Polym. Lett.*, 1964, **2**, 593–596; (*b*) H. E. Swift, J. E. Bozik and C. Y. Wu, *J. Catal.*, 1970, **17**, 331–340; (*c*) W. L. Hsu and A. F. Halasa, *Rubber Chem. Technol.*, 1994, **67**, 82–85.

11 (*a*) C. Bazzini, A. Giarrusso and L. Porri, *Macromol. Rapid Commun.*, 2002, **23**, 922–927; (*b*) C. Bazzini, A. Giarrusso, L. Porri, B. Pirozzi and R. Napolitano, *Polymer*, 2004, **45**, 2871–2275.

12 (*a*) M. Zhao, L. Wang, Q. Mahmood, C. Jing, G. Zhu, X. Zhang, X. Wang and Q. Wang, *Appl. Organomet. Chem.*, 2019, **33**, e4836; (*b*) M. Zhao, X. Zhang, L. Wang, L. Wang, G. Zhu and Q. Wang, *Appl. Organomet. Chem.*, 2022, **36**, e6848; (*c*) M. Zhao, Y. Ma, X. Zhang, L. Wang, G. Zhu and Q. Wang, *Polymers*, 2022, **14**, 3612; (*d*) G. Zhu, X. Zhang, M. Zhao, L. Wang, C. Jing, P. Wang, X. Wang and Q. Wang, *Polymers*, 2018, **10**, 934; (*e*) C. Jing, L. Wang, Q. Mahmood, M. Zhao, G. Zhu, X. Zhang, X. Wang and Q. Wang, *Dalton Trans.*, 2019, **48**, 7862–7874; (*f*) X. Zhang, G. Zhu, Q. Mahmood, M. Zhao, L. Wang, C. Jing, X. Wang and Q. Wang, *J. Polym. Sci., Part A: Polym. Chem.*, 2019, **57**, 767–775; (*g*) C. Jing, L. Wang, G. Zhu, H. Hou, L. Zhou and Q. Wang, *Organometallics*, 2020, **39**, 4019–4026.

13 (*a*) L. K. Johnson, C. M. Killian and M. Brookhart, *J. Am. Chem. Soc.*, 1995, **117**, 6414–6415; (*b*) C. M. Killian, D. J. Tempel, L. K. Johnson and M. Brookhart, *J. Am. Chem. Soc.*, 1996, **118**, 11664–11615; (*c*) B. L. Small, M. Brookhart and A. M. A. Bennett, *J. Am. Chem. Soc.*, 1998, **120**, 4049–4050; (*d*) G. J. P. Britovsek, V. C. Gibson, B. S. Kimberley, P. J. Maddox, S. J. McTavish, G. A. Solan, A. J. P. White and D. J. Williams, *Chem. Commun.*, 1998, **8**, 849–850; (*e*) G. J. P. Britovsek, M. Bruce, V. C. Gibson, B. S. Kimberley, P. J. Maddox, S. Mastroianni, S. J. McTavish, C. Redshaw, G. A. Solan, S. Stromberg, A. J. P. White and D. J. Williams, *J. Am. Chem. Soc.*, 1999, **121**, 8728–8740; (*f*) Y. Zhang, C. Huang, X. Wang, Q. Mahmood, X. Hao, X. Hu, C. Y. Guo, G. A. Solan and W.-H. Sun, *Polym. Chem.*, 2017, **8**, 995; (*g*) Y. Zeng, Q. Mahmood, X. Hao and W.-H. Sun, *J. Polym. Sci., Part A: Polym. Chem.*, 2017, **55**, 1910–1919; (*h*) Y. Zeng, Q. Mahmood, T. Liang and W.-H. Sun, *New J. Chem.*, 2017, **41**, 3653; (*i*) Z. Wang, G. A. Solan, W. Zhang and W.-H. Sun, *Coord. Chem. Rev.*, 2018, **363**, 92–108; (*j*) Q. Mahmood, Y. Zeng, X. Wang, Y. Sun and W.-H. Sun, *Dalton Trans.*, 2017, **46**, 6934–6947; (*k*) Q. Mahmood, Y. Zeng, E. Yue, G. A. Solan, T. Liang and W.-H. Sun, *Polym. Chem.*, 2017, **8**, 6416–6430; (*l*) Z. Wang, G. A. Solan, Q. Mahmood, Q. Liu, Y. Ma, X. Hao and W.-H. Sun, *Organometallics*, 2018, **37**, 380; (*m*) J. Guo, W. Zhang, Q. Mahmood, R. Zhang, Y. Sun and W.-H. Sun, *J. Polym. Sci., Part A: Polym. Chem.*, 2018, **56**, 1269; (*n*) Q. Mahmood, Y. Ma, X. Hao and W.-H. Sun, *Appl. Organomet. Chem.*, 2019, e4857; (*o*) M. Khoshsefat, Y. Ma and W.-H. Sun, *Coord. Chem. Rev.*, 2021, **434**, 213788; (*p*) Q. Mahmood, J. Guo, W. Zhang, Y. Ma, T. Liang and W.-H. Sun, *Organometallics*, 2018, **37**, 957–970; (*q*) Q. Mahmood, E. Yue, J. Guo, W. Zhang, Y. Ma, X. Hao and W.-H. Sun, *Polymer*, 2018, **159**, 124–137; (*r*) Q. Mahmood, X. Li, L. Qin, L. Wang and W.-H. Sun, *Dalton Trans.*, 2022, **51**, 14375–14407; (*s*) M. Qasim, M. S. Bashir, S. Iqbal and Q. Mahmood, *Eur. Polym. J.*, 2021, **160**, 110783; (*t*) Z. Wang, Q. Mahmood, W. Zhang and W.-H. Sun, *Adv. Org. Chem.*, 2023, **79**, 41–86; (*u*) L. Wang, M. Liu, Q. Mahmood, S. Yuan, X. Li, L. Qin, S. Zou, T. Liang and W.-H. Sun, *Eur. Polym. J.*, 2023, **194**, 112112.

14 J. Raynaud, J. Y. Wu and T. Ritter, *Angew. Chem., Int. Ed.*, 2012, **51**, 11805–11808.

15 L. Guo, X. Jing, S. Xiong, W. Liu, Y. Liu, Z. Liu and C. Chen, *Polymers*, 2016, **8**, 389.

16 G. Ricci, G. Leone, G. Zanchin, B. Palucci, A. C. Boccia, A. Sommazzi, F. Masi, S. Zacchini, M. Guelfi and G. Pampaloni, *Macromolecules*, 2021, **54**, 9947–9959.

17 O. H. Hashmi, Y. Champouret and M. Visseaux, *Molecules*, 2019, **24**, 3024.

18 W. Lin, L. Zhang, H. Suo, A. Vignesh, N. Yousuf, X. Hao and W.-H. Sun, *New J. Chem.*, 2020, **44**, 8076–8084.

19 G. Zhu, L. Wang, Q. Mahmood, L. Zhou and Q. Wang, *Polym. Test.*, 2021, **102**, 107317.
20 R. Yuan, G. Ren, Q. Mahmood, Y. Zeng, Y. Wang, T. Liang and W.-H. Sun, *Organometallics*, 2023, **42**, 3307–3318.
21 (*a*) F. Huang, Z. Sun, S. Du, E. Yue, J. Ba, X. Hu, T. Liang, G. B. Galland and W. H. Sun, *Dalton Trans.*, 2015, **44**, 14281–14292; (*b*) R. Zhang, Z. Wang, Z. Flisak, X. Hao, Q. Liu and W.-H. Sun, *J. Polym. Sci., Part A: Polym. Chem.*, 2017, **55**, 2601–2610; (*c*) J. Yu, Y. Zeng, W. Huang, X. Hao and W.-H. Sun, *Dalton Trans.*, 2011, **40**, 8436–8443; (*d*) Y. Zhang, C. Huang, X. Wang, Q. Mahmood, X. Hao, X. Hu, C. Y. Guo, G. A. Solan and W.-H. Sun, *Polym. Chem.*, 2017, **8**, 995–1005.
22 (*a*) J. Li, Q. Zhang, X. Hu, Y. Ma, G. A. Solan, Y. Sun and W.-H. Sun, *Appl. Organomet. Chem.*, 2019, **34**, e5254; (*b*) L. Xua, J. Li, W. Lin, Y. Ma, X. Hua, Z. Flisak and W.-H. Sun, *J. Organomet. Chem.*, 2021, **937**, 121720.
23 (*a*) M. Yankey, C. Obuah, I. A. Guzei, E. Osei-Twum, G. Hearne and J. Darkwa, *Dalton Trans.*, 2014, **43**, 13913–13923; (*b*) M. S. Shongwe, B. A. Al-Rashdi, H. Adams, M. J. Morris, M. Mikuriya and G. R. Hearne, *Inorg. Chem.*, 2007, **46**, 9558–9568.
24 S. Jiang, Y. Zheng, M. Liu, Z. Yu, Y. Ma, G. A. Solan, W. Zhang, T. Liang and W.-H. Sun, *Organometallics*, 2022, **41**, 3197–3211.
25 (*a*) L. Fang, W. Zhao, C. Han, H. Liu, Y. Hu and X. Zhang, *Eur. J. Inorg. Chem.*, 2019, **2019**, 609–616; (*b*) G. Ricci, G. Leone, A. Boglia, A. C. Boccia and L. Zetta, *Macromolecules*, 2009, **42**, 9263–9267; (*c*) B. Liu, X. Wang, Y. Pan, F. Lin, C. Wu, J. Qu, Y. Luo and D. Cui, *Macromolecules*, 2014, **47**, 8524–8530.
26 M. N. Alnajrani and F. S. Mair, *RSC Adv.*, 2015, **5**, 46372–46385.